Anthogorgienes A–O, New Guaiazulene-Derived Terpenoids from a Chinese Gorgonian Anthogorgia Species, and Their Antifouling and Antibiotic Activities

ARTICLE *in* JOURNAL OF AGRICULTURAL AND FOOD CHEMISTRY · DECEMBER 2011

Impact Factor: 2.91 · DOI: 10.1021/jf2040862 · Source: PubMed

5 AUTHORS, INCLUDING:

Dawei Chen
China National Center for Food Safety Risk Ass…
21 PUBLICATIONS **52** CITATIONS
SEE PROFILE

Leen van Ofwegen
Naturalis Biodiversity Center
102 PUBLICATIONS **1,021** CITATIONS
SEE PROFILE

Wenhan Lin
Beijing Medical University
167 PUBLICATIONS **2,206** CITATIONS
SEE PROFILE

JOURNAL OF AGRICULTURAL AND FOOD CHEMISTRY

Article

pubs.acs.org/JAFC

Anthogorgienes A−O, New Guaiazulene-Derived Terpenoids from a Chinese Gorgonian *Anthogorgia* Species, and Their Antifouling and Antibiotic Activities

Dawei Chen,[†] Shanjiang Yu,[‡] Leen van Ofwegen,[§] Peter Proksch,[⊥] and Wenhan Lin*[,†]

[†]State Key Laboratory of Natural and Biomimetic Drugs, Peking University, Beijing 100191, People's Republic of China

[‡]China National Center for Biotechnology Development, Beijing 100036, People's Republic of China

[§]National Museum of Natural History Naturalis, 2300 RA Leiden, The Netherlands

[⊥]Institute of Pharmaceutical Biology and Biotechnology, Heinrich-Heine University, 40225 Duesseldorf, Germany

Supporting Information

ABSTRACT: Fifteen new guaiazulene-based terpenoids designated anthogorgienes A−O (**1**−**15**) were isolated from a Chinese gorgonian *Anthogorgia* sp., together with eight known analogues (**16**−**23**). The structural patterns were classified into monomers, dimers, and trimers, which were supposed to be generated from a precursor guaiazulene and followed by side-chain and nucleus oxidation and oxidative rearrangement. The structures of new compounds were elucidated on the basis of extensive spectroscopic (IR, MS, and 1D and 2D NMR) data analysis. A possible biogenetic relationship of the isolated compounds was postulated. Some of the compounds showed potent antifouling activities against the larval settlement of barnacle *Balanus amphitrite*, whereas their antibiotic activities were also evaluated.

KEYWORDS: *marine gorgonian, Anthogorgia sp., guaiazulene-based terpenoids, anthogorgienes A−O, structural elucidation, antifouling activity, antibiotic activity*

INTRODUCTION

Biofouling emerged as a problem many centuries ago and probably for as long as mankind has been sailing the oceans. It caused serious concern considering its long-ranging impacts on marine structures such as ship hulls and platforms. The most effective antifouling agents such as organotins used to control fouling organisms were recently prohibited for application to ships, due to the severely toxic biocides and lack of degradation in the natural environment.[1,2] Therefore, discovery of new environmentally friendly antifouling agents without biocidal properties is desired. Actually, marine organisms such as sponges and corals protect their own surfaces from fouling by their high anesthetic, repellant, and settlement inhibition properties. Within the marine ecosystem, evolution has allowed for the development of certain antifouling properties.[3] The chemistry behind the sessile, unfouled surfaces of marine organisms is largely being investigated. It is well recognized that marine organisms produced diverse natural products to protect themselves from the harmful process of biofouling and protect the surface of their bodies without causing serious environmental problems.[4−6] On the basis of a literature survey, >70% of potential antifouling marine natural products are derived from sponges, algae, and cnidarians and exhibit not only toxins but also anesthetics, growth-inhibiting, attachment-inhibiting, metamorphosis-inhibiting, and repelling properties. The types of marine natural product antifoulants involved terpenes, acetylenes, steroids, phenols, isothiocyanates, nitrogen-containing compounds, glycerol derivatives, and higher fatty acids, of which the most potent natural product is bufalin, a steroid showing >100 times greater toxicity than tributyltin (TBT) and >6000-fold greater potency with respect to antisettlement activity.[7] During the collection of marine organisms from the South China Sea, we found that gorgorians display diverse colors with clean surfaces. These findings led us to suspect that the secondary metabolites generated by gorgorians possess antifouling property. Guaiazulene-based analogues are well recognized for their distinctive blue and purple colors, which are a part of the origin of the brilliant colors of gorgonians and other organisms. Guaiazulene and related derivatives are a class of typical natural products mainly found from gorgonian genera *Calicogorgia*, *Acalycigorgia*, *Euplexaura*, *Alcyonium*, and *Paramuricea*[7−20] and also from some terrestrial plants including the fungal genus *Lactarius*. This sesquiterpene family together with their dimeric or trimeric analogues features an azulene core with various oxidations and ring rearrangements. To date, a few naturally occurring guaiazulenyl dimers have been found from marine gorgonians, whereas fungi and yarrow derive only "mono" guaiazulenyl analogues. A number of dimeric and trimeric products are derived from guaiazulene through oxidative condensation.[21,22] Part of these compounds possess significant biological activities including antibiotic, cytotoxic, and immunoregulating activities as well as inhibitory activities against cell division of fertilized sea urchin and ascidian eggs. In the course of our studies on the chemical diversity of Chinese gorgonians, we examined the lipophilic extract of a species unidentified gorgonian *Anthogorgia* sp., which inhabits Weizhou Island of the

Received: October 11, 2011
Revised: December 7, 2011
Accepted: December 7, 2011
Published: December 7, 2011

dx.doi.org/10.1021/jf2040862 | *J. Agric.Food Chem.* 2012, 60, 112−123

South China Sea. In this paper, the structural elucidation of new guaiazulene-derived analogues, namely, anthogorgienes A−O (**1**−**15**), and the antifouling and antibiotic activities of some of the isolated compounds are reported.

MATERIALS AND METHODS

General Methods. Optical rotations were measured using an Autopol III automatic polarimeter (Rudolph Research Co.). IR spectra were recorded on a Thermo Nicolet Nexus 470 FT-IR spectrometer. NMR spectra were measured on a Bruker Avance-500 FT NMR spectrometer (500 MHz) and a Bruker Avance-600 FT NMR spectrometer using TMS as the internal standard. HRESIMS spectra were obtained on a Thermo Scientific LTQ Orbitrap XL spectrometer. CD spectra were measured on a JASCO J-810 spectropolarimeter. Column chromatography was performed on silica gel (200−300 mesh). The HF_{254} silica gel for TLC was provided by Sigma Co. Ltd. Sephadex LH-20 (18−110 μm) was obtained from Pharmacia Co., and ODS (50 μm) was provided by YMC Co. High-performance liquid chromatography (HPLC) was performed on an Alltech 426 apparatus with a 3300-ELSD UV detector. A Kromasil prepacked column (ODS, 10 mm × 250 mm, for reversed-phase) and a chiral column (OD-RH, 4.6 mm × 150 mm) were used in the HPLC separation.

Animal Material. Fresh gorgonian *Anthogorgia* sp. was collected from the inner coral reef at a depth of around 10 m in Northern Bay (Weizhou Island), Guangxi Province, People's Republic of China, in June 2009, and the sample was immediately frozen after collection. The specimen was identified by Dr. Leen van Ofwegen (National Museum of National History Naturalis, The Netherlands). A voucher specimen (GWB-55) was deposited at State Key Laboratory of Natural and Biomimetic Drugs, Peking University.

Extraction and Isolation. The frozen gorgonian (780 g, wet weight) was homogenized and extracted with MeOH (2.0 L × 3). The concentrated extract was desalted by dissolving in MeOH (400 mL) to obtain a residue (29.0 g) that was further partitioned between H_2O (150 mL) and EtOAc (100 mL). The EtOAc fraction was concentrated under vacuum to afford a residue (4.9 g), which was subjected to Si gel VLC (vacuum liquid chromatography) (6.0 × 5.5 cm, 200−300 mesh) and eluted with a gradient of petroleum ether/acetone (50:1−10:1) to collect 10 fractions (F1−F10). F4 (978.8 mg, 30:1) displayed the ^{1}H NMR features of diverse guaiazulenyl analogues. This fraction was fractionated upon a Si gel column (2.0 × 10 cm) and eluted with petroleum ether/EtOAc (5:1) to get six subfractions (SF1−SF6). SF1 (634 mg) was further fractionated on a Sephadex LH-20 column (18 μm, 3 × 50 cm) using CH_2Cl_2/MeOH (1:1) as an eluent to give **16** (500 mg), **20** (17.3 mg), and **21** (8.6 mg). SF2 (35 mg) was purified by semipreparative HPLC (2 × 20 cm, 5.0 μm) using a mobile phase of MeOH/H_2O (4:1) to give **10** (2.2 mg), **11** (2.2 mg), and **13** (2.3 mg). SF3 (83 mg) was fractionated upon semipreparative HPLC (mobile phase, MeCN/H_2O = 85:15) to obtain **22** (7.5 mg), **23** (25.2 mg), **2** (3.1 mg), **3** (1.6 mg), **4** (1.8 mg), **5** (1.6 mg), and **6** (3.5 mg). SF4 (28 mg) was purified by semipreparative HPLC (mobile phase, MeCN/H_2O = 9:1) to give **12** (1.5 mg) and a mixture containing **14** and **15** (5.2 mg). This mixture was further separated on an OD-RH column eluting with a mobile phase of MeCN/H_2O (92.8) to obtain **14** (2.6 mg) and **15** (2.2 mg). SF5 (73 mg) was fractionated upon semipreparative HPLC (mobile phase, MeCN/H_2O = 4:1) to give **7** (5.1 mg), **8** (2.1 mg), **1** (1.2 mg), and **9** (1.3 mg), whereas SF6 (55 mg) was separated upon semipreparative HPLC (mobile phase, MeCN/H_2O = 7:3) to afford **17** (2.1 mg), **18** (1.6 mg), and **19** (3.8 mg).

*Anthogorgiene A (**1**):* pale yellow oil; $[\alpha]_D^{20}$ +36.7 (*c* 0.075, MeOH); UV (MeOH) λ_{max} 249, 260, 311 nm; IR (KBr) ν_{max} 1711, 1689, 1631, 1458, 1379, 1058 cm^{-1}; ^{1}H and ^{13}C NMR data, see Tables 1 and 2; positive HRESIMS *m*/*z* 231.1374 $[M + H]^+$ (calcd for $C_{15}H_{19}O_2$, 231.1385).

*Anthogorgiene B (**2**):* purple amorphous powder; UV (MeOH) λ_{max} 246, 286, 346, 530 nm; IR (KBr) ν_{max} 1702, 1680, 1617, 1543, 1435, 1370, 1166 cm^{-1}; ^{1}H and ^{13}C NMR data, see Tables 1 and 2; positive HRESIMS *m*/*z* 405.1813 $[M + Na]^+$ (calcd for $C_{27}H_{27}O_2Na$, 405.1830).

*Anthogorgiene C (**3**):* purple amorphous powder; UV (MeOH) λ_{max} 247, 289, 349, 522 nm; IR (KBr) ν_{max} 1700, 1593, 1440, 1382, 1167 cm^{-1}; ^{1}H and ^{13}C NMR data, see Tables 1 and 2; positive HRESIMS *m*/*z* 425.2462 $[M + H]^+$ (calcd for $C_{30}H_{33}O_2$, 425.2481).

*Anthogorgiene D (**4**):* purple amorphous powder; UV (MeOH) λ_{max} 250, 292, 348, 492 nm; IR (KBr) ν_{max} 1701, 1599, 1546, 1454, 1377, 1164, 1119, 1070 cm^{-1}; ^{1}H and ^{13}C NMR data, see Tables 1 and 2; positive HRESIMS *m*/*z* 471.2891 $[M + H]^+$ (calcd for $C_{32}H_{39}O_3$, 471.2899).

*Anthogorgiene E (**5**):* purple amorphous powder; UV (MeOH) λ_{max} 248, 288, 352, 523 nm; IR (KBr) ν_{max} 1702, 1652, 1546, 1456, 1431, 1374, 1247, 1163 cm^{-1}; ^{1}H and ^{13}C NMR data, see Tables 1 and 2; positive HRESIMS *m*/*z* 425.2464 $[M + H]^+$ (calcd for $C_{30}H_{33}O_2$, 425.2481).

*Anthogorgiene F (**6**):* green amorphous powder; UV (MeOH) λ_{max} 246, 289, 373 nm; IR (KBr) ν_{max} 1718, 1666, 1630, 1546, 1436, 1380, 1282, 1133, 1070 cm^{-1}; ^{1}H and ^{13}C NMR data, see Tables 1 and 2; positive HRESIMS *m*/*z* 457.2722 $[M + H]^+$ (calcd for $C_{31}H_{37}O_3$, 457.2743).

*Anthogorgiene G (**7**):* green amorphous powder; UV (MeOH) λ_{max} 242, 288, 389 nm; IR (KBr) ν_{max} 1743, 1655, 1544, 1457, 1432, 1376, 1150, 1066 cm^{-1}; ^{1}H and ^{13}C NMR data, see Tables 1 and 2; positive HRESIMS *m*/*z* 443.2563 $[M + H]^+$ (calcd for $C_{30}H_{35}O_3$, 443.2586).

*Anthogorgiene H (**8**):* green amorphous powder; UV (MeOH) λ_{max} 242, 289, 394 nm; IR (KBr) ν_{max} 1767, 1654, 1545, 1462, 1430, 1379, 1302, 1165, 1057 cm^{-1}; ^{1}H and ^{13}C NMR data, see Tables 1 and 2; positive HRESIMS *m*/*z* 457.2721 $[M + H]^+$ (calcd for $C_{31}H_{37}O_3$, 457.2743).

*Anthogorgiene I (**9**):* yellow amorphous powder; $[\alpha]_D^{20}$ +1.34 (*c* 0.4, MeOH); UV (MeOH) λ_{max} 254, 322 nm; IR (KBr) ν_{max} 1711, 1687, 1596, 1517, 1459, 1380, 1224, 1142, 1022 cm^{-1}; ^{1}H and ^{13}C NMR data, see Tables 1 and 2; positive HRESIMS *m*/*z* 479.2192 $[M + Na]^+$ (calcd for $C_{30}H_{33}O_4Na$, 479.2198).

*Anthogorgiene J (**10**):* purple amorphous powder; UV (MeOH) λ_{max} 249, 288, 347, 528 nm; IR (KBr) ν_{max} 1706, 1682, 1590, 1548, 1504, 1457, 1370, 1157, 1093, 1020 cm^{-1}; ^{1}H and ^{13}C NMR data, see Tables 3 and 4; positive HRESIMS *m*/*z* 579.3259 $[M + H]^+$ (calcd for $C_{42}H_{43}O_2$, 579.3263).

*Anthogorgiene K (**11**):* purple amorphous powder; UV (MeOH) λ_{max} 250, 289, 351, 492 nm; IR (KBr) ν_{max} 1701, 1628, 1546, 1463, 1440, 1373, 1161, 1109, 1053 cm^{-1}; ^{1}H and ^{13}C NMR data, see Tables 3 and 4; positive HRESIMS *m*/*z* 625.3668 $[M + H]^+$ (calcd for $C_{44}H_{49}O_3$, 625.3682).

*Anthogorgiene L (**12**):* purple amorphous powder; UV (MeOH) λ_{max} 249, 289, 351, 492 nm; IR (KBr) ν_{max} 3305, 1696, 1597, 1547, 1457, 1367, 1022, 872 cm^{-1}; ^{1}H and ^{13}C NMR data, see Tables 3 and 4; positive HRESIMS *m*/*z* 609.3729 $[M + H]^+$ (calcd for $C_{44}H_{49}O_2$, 609.3733).

*Anthogorgiene M (**13**):* purple amorphous powder; UV (MeOH) λ_{max} 250, 291, 350, 509 nm; IR (KBr) ν_{max} 1696, 1630, 1601, 1547, 1373, 1165, 1059 cm^{-1}; ^{1}H and ^{13}C NMR data, see Tables 3 and 4; positive HRESIMS *m*/*z* 621.3757 $[M + H]^+$ (calcd for $C_{45}H_{49}O_2$, 621.3733).

*Anthogorgiene N (**14**):* flavo-green amorphous powder; $[\alpha]_D^{20}$ +842.8 (*c* 0.04, MeOH); UV (MeOH) λ_{max} 246, 289, 349, 430 nm; IR (KBr) ν_{max} 1707, 1632, 1457, 1434, 1371, 1162, 1063 cm^{-1}; ^{1}H and ^{13}C NMR data, see Tables 3 and 4; positive HRESIMS *m*/*z* 623.3869 $[M + H]^+$ (calcd for $C_{45}H_{51}O_2$, 623.3889).

*Anthogorgiene O (**15**):* flavo-green amorphous powder; $[\alpha]_D^{20}$ −950.3 (*c* 0.04, MeOH); UV (MeOH) λ_{max} 246, 289, 349, 430 nm; IR (KBr) ν_{max} 1707, 1601, 1545, 1457, 1432, 1376, 1150, 1066 cm^{-1}; ^{1}H and ^{13}C NMR data, see Tables 3 and 4; positive HRESIMS *m*/*z* 623.3864 $[M + H]^+$ (calcd for $C_{45}H_{51}O_2$, 623.3889).

Larval Settlement Bioassays. Adults of the barnacle *Balanus amphitrite* Darwin were exposed to air for >6 h and then were placed in a container filled with fresh 0.22 μm filtered seawater (FSW) to release nauplii. The collected nauplii were reared to cyprid stage

dx.doi.org/10.1021/jf2040862 | J. Agric.Food Chem. 2012, 60, 112−123

Table 1. ^{1}H NMR Data for Anthogorgienes A–I (1–9)

no.	1[a]	2[a]	3[a]	4[b]	5[a]	6[a]	7[a]	8[a]	9[a]
2	2.34 dd (3.7, 19.0)								3.14 d (19.0)
	2.99 dd (7.7, 19.0)								2.78 d (19.0)
3	3.44 m								
4	7.86 brs	10.66 s		7.17 s		7.75 d (1.4)	7.32 brs	7.12 d (1.9)	7.50 brs
6		7.88 d (8.3)	7.26 d (8.3)		7.65 d (7.5)	7.22 dd (1.4, 7.8)	7.25 brd (7.5)	7.21 dd (1.9, 7.5)	
7	7.66 brs	7.16 d (8.3)	7.07 d (8.3)	5.58 s	7.47 d (7.5)	7.13 d (7.8)	7.20 d (7.5)	7.15 d (7.5)	7.57 brs
11	3.59 dq (6.9, 6.9)		3.32 dq (6.8, 6.8)	3.72 dq (6.8, 6.8)	4.21 dq (6.8, 6.8)	2.95 dq (6.8, 6.8)	2.83 dq (6.8, 6.8)	2.83 dq (6.8, 6.8)	3.55 dq (6.9, 6.9)
12	1.25 d (6.9)		1.28 d (6.8)	1.22 d (6.8)	1.36 d (6.8)	1.27 d (6.8)	1.17 d (6.8)	1.17 d (6.8)	1.23 d (6.9)
13	1.25 d (6.9)		1.28 d (6.8)	1.23 d (6.8)	1.36 d (6.8)	1.28 d (6.8)	1.17 d (6.8)	1.16 d (6.8)	1.23 d (6.9)
14	1.45 d (7.1)	2.41 s	1.97 s	2.09 s	2.00 s	1.85 s	1.73 s	1.68 s	1.87 s
15	2.71 s	2.67 s	2.62 s	2.60 s	2.67 s	2.47 s	2.24 s	2.04 s	2.77 s
2′		7.44 s	7.43 s	7.40 s	7.41 s	7.31 s	5.95 s	5.87 s	
4′		8.21 brs	8.18 brs	8.17 d (1.7)	8.22 brs	8.13 d (1.7)	8.15 d (1.7)	8.14 d (1.7)	7.74 brs
6′		7.43 brd (10.8)	7.39 brd (10.8)	7.48 dd (1.7, 10.8)	7.40 brd (10.8)	7.40 dd (1.7, 10.8)	7.49 dd (1.7, 10.8)	7.47 dd (1.7, 10.8)	
7′		7.02 d (10.8)	6.97 d (10.8)	6.98 d (10.8)	6.98 d (10.8)	7.07 d (10.8)	7.15 d (10.8)	7.13 d (10.8)	7.70 brs
11′		3.11 dq (6.8, 6.8)	3.09 dq (6.8, 6.8)	3.12 dq (6.8, 6.8)	3.11 dq (6.8, 6.8)	3.08 dq (6.8, 6.8)	3.10 dq (6.8, 6.8)	3.09 dq (6.8, 6.8)	3.55 dq (6.9, 6.9)
12′		1.40 d (6.8)	1.39 d (6.8)	1.34 d (6.8)	1.39 d (6.8)	1.37 d (6.8)	1.38 d (6.8)	1.38 d (6.8)	1.23 d (6.9)
13′		1.40 d (6.8)	1.39 d (6.8)	1.34 d (6.8)	1.39 d (6.8)	1.37 d (6.8)	1.38 d (6.8)	1.37 d (6.8)	1.23 d (6.9)
14′		2.68 s	2.67 s	2.62 s	2.69 s	2.55 s	2.37 s	2.38 s	2.11 s
15′		2.68 s	2.68 s	2.57 s	2.60 s	2.99 s	2.87 s	2.88 s	2.50 s
MeO				3.38 s		3.56 s		3.47 s	
				3.39 s					

[a]Measured in $CDCl_3$. [b]Measured in DMSO-d_6.

dx.doi.org/10.1021/jf2040862 | J. Agric.Food Chem. 2012, 60, 112–123

Table 2. ^{13}C NMR Data for Anthogorgienes A–I (1–9)

no.	1[a]	2[a]	3[a]	4[b]	5[a]	6[a]	7[a]	8[a]	9[a]
1	207.0 qC	197.3 qC	198.3 qC	198.4 qC	188.0 qC	198.3 qC	107.1 qC	110.8 qC	205.5 qC
2	46.2 CH_2	140.2 qC	138.3 qC	136.3 qC	144.0 qC	131.4 qC	159.4 qC	160.8 qC	53.8 CH_2
3	32.3 CH	151.4 qC	153.0 qC	152.8 qC	147.0 qC	149.6 qC	127.7 qC	127.7 qC	42.4 qC
4	122.3 CH	189.5 CH	145.8 qC	116.4 CH	131.7 qC	129.0 CH	127.4 CH	128.1 CH	122.0 CH
5	204.7 qC	129.4 qC	209.0 qC	154.4 qC	149.6 qC	145.6 qC	146.8 qC	146.5 qC	204.1 qC
6	140.9 qC	131.1 CH	130.0 CH	135.1 qC	131.1 CH	129.4 CH	127.4 CH	127.0 CH	140.6 qC
7	129.1 CH	132.2 CH	131.3 CH	103.7 CH	137.0 CH	131.8 CH	132.7 CH	132.6 CH	129.9 CH
8	138.9 qC	142.5 qC	138.6 qC	136.5 qC	138.7 qC	137.3 qC	133.9 qC	133.7 qC	138.9 qC
9	136.7 qC	128.0 qC	128.4 qC	125.0 qC	131.4 qC	135.8 qC	134.7 qC	134.6 qC	135.4 qC
10	160.9 qC	148.7 qC	144.2 qC	146.7 qC	189.3 qC	168.6 qC	172.9 qC	173.1 qC	162.7 qC
11	36.1 CH		40.2 CH	29.2 CH	29.1 CH	33.6 CH	33.8 CH	33.7 CH	35.8 CH
12	19.0 CH_3		18.4 CH_3	24.0 CH_3	24.6 CH_3	23.9 CH_3	23.7 CH_3	23.8 CH_3	19.0 CH_3
13	19.1 CH_3		18.5 CH_3	23.9 CH_3	24.7 CH_3	24.0 CH_3	23.7 CH_3	24.1 CH_3	19.1 CH_3
14	21.5 CH_3	18.5 CH_3	15.7 CH_3	12.6 CH_3	15.0 CH_3	17.0 CH_3	9.9 CH_3	9.8 CH_3	29.6 CH_3
15	18.4 CH_3	17.8 CH_3	17.3 CH_3	13.7 CH_3	23.2 CH_3	21.0 CH_3	20.8 CH_3	20.7 CH_3	18.5 CH_3
1′		115.6 qC	116.2 qC	117.2 qC	119.3 qC	120.6 qC	115.2 qC	115.4 qC	197.8 qC
2′		139.6 CH	139.7 CH	140.0 CH	138.8 CH	137.6 CH	137.8 CH	138.0 CH	136.5 qC
3′		138.9 qC	138.7 qC	138.3 qC	138.5 qC	138.3 qC	138.8 qC	138.3 qC	147.0 qC
4′		133.8 CH	133.5 CH	133.9 CH	134.0 CH	133.7 CH	133.7 CH	133.6 CH	116.2 CH
5′		141.1 qC	140.6 qC	140.7 qC	140.8 qC	140.8 qC	141.6 qC	141.2 qC	204.4 qC
6′		135.3 CH	135.1 CH	135.6 CH	135.2 CH	135.3 CH	135.3 CH	135.1 CH	139.9 qC
7′		127.7 CH	127.4 CH	127.4 CH	127.3 CH	127.8 CH	128.6 CH	128.2 CH	133.1 CH
8′		145.7 qC	145.8 qC	145.8 qC	145.0 qC	146.6 qC	146.1 qC	146.3 qC	139.1 qC
9′		135.7 qC	135.5 qC	135.3 qC	134.3 qC	133.9 qC	134.8 qC	134.9 qC	136.5 qC
10′		125.0 qC	124.8 qC	124.5 qC	125.0 qC	124.9 qC	124.5 qC	124.4 qC	152.7 qC
11′		38.0 CH	37.9 CH	37.5 CH	38.0 CH	37.9 CH	37.9 CH	37.9 CH	36.0 CH
12′		24.6 CH_3	24.6 CH_3	24.9 CH_3	23.7 CH_3	24.6 CH_3	24.6 CH_3	24.6 CH_3	19.0 CH_3
13′		24.6 CH_3	24.6 CH_3	24.9 CH_3	24.1 CH_3	24.6 CH_3	24.6 CH_3	24.6 CH_3	19.1 CH_3
14′		12.9 CH_3	12.9 CH_3	13.1 CH_3	13.0 CH_3	12.9 CH_3	12.6 CH_3	12.6 CH_3	13.0 CH_3
15′		25.8 CH_3	25.7 CH_3	25.4 CH_3	25.9 CH_3	25.7 CH_3	25.6 CH_3	25.6 CH_3	17.1 CH_3
OMe				55.9 CH_3		51.8 CH_3		52.9 CH_3	
				56.0 CH_3					

[a]Measured in $CDCl_3$. [b]Measured in DMSO-d_6.

according to the method described by Thiyagarajan et al.[23] Larvae were fed by *Chaetoceros gracilis* under 26 °C and developed to cyprids within 4 days. Fresh cyprids were used in the tests. Adults of *Bugula neritina* were collected from submerged rafts at the fish farms in Yung Shue-O, Hong Kong (114° 21′ E, 22° 24′ N), and larvae were obtained according to the method described by Dobretsov.[24]

Antibiotic Test. Antibacterial and antifungal bioassays were conducted in triplicate by following the National Center for Clinical Laboratory Standards (NCCLS) recommendations.[25] The bacterial strains *Staphylococcus aureus* (CGMCC 1.2465) and *Streptococcus pneumoniae* (CGMCC 1.1692) were grown on Mueller–Hinton agar, and the fungi *Aspergillus fumigatus* (CGMCC 3.5835), *Aspergillus flavus* (CGMCC 3.0951), and *Aspergillus oxysporum* (CGMCC 3.2830) were grown on potato dextrose agar. Targeted microbes (3–4 colonies) were prepared from broth culture (bacteria, 37 °C for 24 h; fungus, 28 °C for 48 h), and the final spore suspensions of bacteria (in MHB medium) and fungus (in PDB medium) were 10^6 cells/mL and 10^4 mycelial fragments/mL, respectively. Test samples (10 mg/mL as stock solution in DMSO and serial dilutions) were transferred to a 96-well clear plate in triplicate, and the suspension of the test organisms was added to each well, achieving a final volume of 200 μL (antimicrobial ampicillin and amphotericin B were used as the positive controls). After incubation, the absorbance at 595 nm was measured with a microplate reader (TECAN), and the inhibition rate was calculated and plotted versus test concentrations to afford the IC_{50}.

RESULTS AND DISCUSSION

The frozen gorgonian *Anthogorgia* sp. was homogenized and extracted with MeOH immediately. The EtOAc-soluble fraction from the MeOH extract was detected by ^1H NMR spectrum, which showed diverse guaiazulenyl features. Thus, this fraction was repeatedly separated upon column chromatography including semipreparative HPLC to yield 23 compounds. Those compounds are classified into three patterns, involving monomers, dimers, and trimers.

Monomers were determined as anthogorgiene A (**1**), guaiazulene (GA) (**16**), guaiazulene-3,5-dione (**17**), ketolactone (**18**), and formylguaiazulene (**19**) (Figure 1). Guaiazulene was isolated as a principal pigment in the specimen and also as a main component from other corals.[9] It was a U.S. FDA-approved cosmetic color additive of some skin care products. Guaiazulene-3,5-dione (**17**) was reported to be derived from guaiazulene by autoxidation,[23] whereas formylguaiazulene was also derived from GA under selenium dioxide.[24] Ketolactone (**18**) was reported to be an artifact derived from linderazulene, but Scheuer et al. isolated it from a deep sea gorgonian and strongly indicated it being a genuine natural product.[11]

Anthogorgiene A (**1**) was obtained as a pale yellow oil. Its HRESIMS afforded an ion peak at m/z 231.1374 $[M + H]^+$, which was in accordance with a molecular formula of $C_{15}H_{18}O_2$. The IR spectrum showed absorptions for carbonyl groups (1711, 1689 cm^{-1}) and olefinic bonds (1631 cm^{-1}). ^{13}C NMR and APT spectra displayed a total of 15 resonances, including 6 phenyl carbons, 4 methyls, 2 ketones, 2 aliphatic methines, and a methylene, whereas HSQC assigned all protonated carbons.

dx.doi.org/10.1021/jf2040862 | J. Agric.Food Chem. 2012, 60, 112–123

Table 3. ^{1}H NMR Data for Anthogorgienes J−O (10−15) (500 MHz, *J* in Hz)

no.	10[a]	11[a]	12[a]	13[b]	14[a]	15[a]
4	10.70 s	5.87 s		7.03 s	6.19 s	6.15 s
6	7.84 s	7.39 s	7.27 s		5.96 d (11.2)	6.00 d (11.2)
7				7.48 s	5.09 d (11.2)	5.05 d (11.2)
11				3.19 dq (6.8, 6.8)	2.32 dq (6.8, 6.8)	2.32 dq (6.8, 6.8)
12			1.74 s	1.23 d (6.8)	1.05 d (6.8)	1.05 d (6.8)
13			1.74 s	1.25 d (6.8)	1.05 d (6.8)	1.05 d (6.8)
14	2.46 s	2.30 s	2.54 s	2.17 s	2.30 s	2.26 s
15	2.41 s	2.21 s	2.33 s	2.46 s	1.60 s	1.60 s
2′	7.45 s	7.43 s	7.482 s	7.44 s	7.53 s	7.49 s
4′	8.22 brs	8.19 d (1.5)	8.18 d (1.5)	8.18 brs	8.21 d (1.9)	8.21 d (1.9)
6′	7.44 brd (10.8)	7.49 dd (1.5, 10.8)	7.41 dd (1.5, 10.8)	7.39 brd (10.8)	7.41 dd (1.9, 10.8)	7.41 dd (1.9, 10.8)
7′	7.03 d (10.8)	7.01 d (10.8)	6.96 d (10.8)	6.96 d (10.8)	6.99 d (10.8)	7.05 d (10.8)
11′	3.12 dq (6.8, 6.8)	3.13 dq (6.9, 6.9)	3.13 dq (6.9, 6.9)	3.10 dq (6.8, 6.8)	3.10 dq (6.8, 6.8)	3.10 dq (6.8, 6.8)
12′	1.41 d (6.8)	1.35 d (6.9)	1.39 d (6.9)	1.39 d (6.8)	1.39 d (6.8)	1.39 d (6.8)
13′	1.41 d (6.8)	1.35 d (6.9)	1.39 d (6.9)	1.39 d (6.8)	1.39 d (6.8)	1.39 d (6.8)
14′	2.71 s	2.62 s	2.68 s	2.68 s	2.69 s	2.71 s
15′	2.74 s	2.63 s	2.74 s	2.71 s	2.81 s	2.73 s
2″	7.49 s	7.48 s	7.48 s	6.19 s	7.56 s	7.42 s
4″	8.25 brs	8.23 d (1.5)	8.25 d (1.5)	7.23 s	8.10 d (1.9)	8.10 d (1.9)
6″	7.43 brd (10.8)	7.47 dd (1.5, 10.8)	7.38 dd (1.5, 10.8)		7.33 dd (1.9, 10.8)	7.33 dd (1.9, 10.8)
7″	6.94 d (10.8)	6.96 d (10.8)	6.94 d (10.8)	10.80 s	6.95 d (10.8)	6.94 d (10.8)
11″	3.12 dq (6.8, 6.8)	3.13 dq (6.9, 6.9)	3.13 dq (6.9, 6.9)	3.73 dq (6.8, 6.8)	3.06 dq (6.8, 6.8)	3.06 dq (6.8, 6.8)
12″	1.40 d (6.8)	1.35 d (6.9)	1.40 d (6.9)	1.39 d (6.8)	1.37 d (6.8)	1.37 d (6.8)
13″	1.40 d (6.8)	1.35 d (6.9)	1.40 d (6.9)	1.39 d (6.8)	1.37 d (6.8)	1.37 d (6.8)
14″	2.69 s	2.64 s	2.72 s	2.19 s	2.56 s	2.63 s
15″	2.40 s	2.32 s	2.41 s	2.89 s	3.12 s	3.11 s
OCH_3		3.29 s, 3.31s				

[a]Measured in $CDCl_3$. [b]Measured in DMSO-d_6.

On the basis of 2D NMR analysis, an indanone nucleus was established. The ^{1}H−^{1}H COSY correlations of meta-coupling H-4 (δ_H 7.86) and H-7 (δ_H 7.66) and the NOE relationship between H-4 and H-3 indicated C-6 and C-8 to be substituted. The presence of an isobutanoyl group was recognized from the ^{1}H−^{1}H COSY correlations between a methine proton (δ_H 3.59) and two methyl protons, which were overlapped at δ_H 1.25, together with the HMBC interaction between the methyl protons and a ketone (δ_C 204.7, C-5). The linkage of the isobutanoyl group to C-6 was deduced by the HMBC interactions from H-4 and H-7 to C-5. Finally, a methyl substitution at C-8 was confirmed by the NOE relationship between H_3-15 (δ_H 2.71) and H-7 in addition to their HMBC data. In regard to the sole asymmetric center C-3, the sign of rotation reflected its configuration.[26] Because the absolute configuration of the similar structure dextrorotatory 3,7-dimethylindanone was unequivocally determined to be *S* in contrast to the *R* configuration of levorotatory 3-methylindanone,[27] the rotation sign (+36.7) of **1** was thus in agreement with 3*S*. As shown in Scheme 1, **1** was depicted to be derived from guaiazulene via a C-1 and C-5 peroxidated intermediate to follow a 4,5,6-cyclopropane formation and then cleavage of the C-4/C-5 bond.

Semipreparative HPLC separation of the same fraction led to the isolation of 12 guaiazulene-bearing dimers, involving 8 new analogues designated anthogorgienes B−I (**2**−**9**) (Figure 2). Four known analogues were identical to 2,2′-diguaiazulenylmethane (**20**), 2,2′-biguaiazulenyl (**21**), and indenones **22** and **23**. Compounds **20** and **21** were formerly isolated from gorgonian *Calicogorgia granulose*[10] and deep sea gorgonian *Pseudothesia* sp., whereas **22** and **23** were reported to be derived from autoxidation of guaiazulene in DMF at high temperature.[24]

Anthogorgiene B (**2**) was obtained as a purple powder with the molecular formula $C_{27}H_{26}O_2$, which was determined by HRESIMS (*m*/*z* 405.1813 [M + Na]$^+$, calcd 405.1830), indicating 15° unsaturation. The UV bands at 246, 286, 346, and 530 nm, along with the IR absorptions at 1702 and 1680 cm^{-1}, suggested the presence of carbonyl and conjugated polyene (or phenyl) groups. The ^{1}H NMR spectrum of **2** exhibited an aldehydic proton (δ_H 10.66, s), an ABX spin system at δ_H 8.21 (brs), 7.43 (brd, *J* = 10.8 Hz), and 7.02 (d, *J* = 10.8 Hz), an AB spin system at δ_H 7.88 (d, *J* = 8.3 Hz), 7.16 (d, *J* = 8.3 Hz), and a singlet at δ_H 7.44 (s), in addition to four methyl singlets (δ_H 2.68, 2.68, 2.67, 2.41). An aliphatic methine δ_H 3.11 (1H, dq, *J* = 6.8 Hz) coupled to two methyl doublets at δ_H 1.40 (6H, d, *J* = 6.8 Hz) was attributed to an isopropyl group. The APT spectrum exhibited a total of 27 carbons, including 18 sp^2 signals together with an aldehydic and a ketone carbon. These NMR data (Tables 1 and 2) featured a guaiazulene-bearing indenone, closely related to **22**. Analysis of 2D NMR spectra (^{1}H−^{1}H COSY, HMQC, HMBC, and NOESY) revealed that **2** differed from **22** due to the substituents bearing at indenone unit. The presence of a phenyl AB spin system for H-6 (δ_H 7.88, d, *J* = 8.3 Hz) and H-7 (δ_H 7.16, d, *J* = 8.3 Hz), in association with the HMBC interactions from H-6 to the methyl carbon C-15 (δ_C 17.8) and C-5 (δ_C 129.4) and from H-7 to the aldehydic carbon C-4 (δ_C 189.5) and C-8 (δ_C 142.5), clarified the substitution of the aldehydic group at C-5, whereas a methyl group was positioned at C-8. These assignments were also supported by the observation of NOE interactions between H_3-15 (δ_H 2.67)/H-7, H-6/H-4 (δ_H 10.66, s), in addition to the NOE interaction between H-4 and H_3-14 (δ_H 2.41, s).

dx.doi.org/10.1021/jf2040862 | J. Agric.Food Chem. 2012, 60, 112−123

Table 4. ^{13}C NMR Data of for Anthogorgienes J−O (10−15)

no.	10[a]	11[b]	12[a]	13[b]	14[a]	15[a]
1	197.9 qC	198.7 qC	198.7 qC	198.6 qC	199.0 qC	198.7 qC
2	140.3 qC	136.9 qC	136.9 qC	136.4 qC	142.7 qC	142.9 qC
3	151.4 qC	154.7 qC	154.7 qC	152.1 qC	161.8 qC	162.6 qC
4	190.0 CH	99.8 CH		113.9 CH	123.8 CH	123.9 CH
5	128.3 qC	142.0 qC	142.0 qC	152.2 qC	139.3 qC	139.3 qC
6	132.5 CH	133.6 CH	133.0 CH	137.0 qC	128.2 CH	128.5 CH
7	128.3 qC	127.6 qC	127.6 qC	129.2 CH	45.6 CH	45.7 CH
8	142.7 qC	136.2 qC	136.2 qC	136.1 qC	80.3 qC	80.4 qC
9	127.9 qC	129.4 qC	129.4 qC	125.3 qC	65.8 qC	65.9 qC
10	146.9 qC	143.5 qC	143.5 qC	146.7 qC	138.8 qC	138.8 qC
11			72.7 qC	31.2 CH	36.3 CH	36.0 CH
12			33.0 CH_3	22.8 CH_3	21.7 CH_3	21.8 CH_3
13			33.0 CH_3	23.0 CH_3	22.4 CH_3	22.4 CH_3
14	18.45 CH_3	16.3 CH_3	19.8 CH_3	12.4 CH_3	13.5 CH_3	13.6 CH_3
15	15.85 CH_3	15.3 CH_3	15.2 CH_3	15.5 CH_3	18.4 CH_3	18.3 CH_3
1′	115.9 qC	117.qC	117.1 qC	116.9 qC	116.7 qC	116.9 qC
2″	139.3 CH	140.2 CH	139.5 CH	139.6 CH	139.7 CH	138.8 CH
3′	124.6 qC	124.6 qC	124.6 qC	124.7 qC	125.2 qC	124.6 qC
4′	133.8 CH	133.9 CH	133.4 CH	133.5 CH	133.8 CH	133.8 CH
5′	141.06 qC	140.7 qC	140.7 qC	140.4 qC	141.0 qC	140.9 qC
6′	135.3 CH	135.7 CH	135.1 CH	135.0 CH	135.1 CH	135.4 CH
7′	127.7 CH	127.5 CH	127.0 CH	127.1 CH	127.5 CH	127.6 CH
8′	145.8 qC	145.7 qC	145.7 qC	145.8 qC	145.2 qC	146.8 qC
9′	135.8 qC	135.2 qC	135.2 qC	135.3 qC	135.6 qC	134.7 qC
10′	138.9 qC	138.4 qC	138.4 qC	138.5 qC	138.9 qC	138.9 qC
11′	37.9 CH	37.5 CH	37.5 CH	37.9 CH	37.9 CH	37.9 CH
12′	24.7 CH_3	24.9 CH_3	24.7 CH_3	24.7 CH_3	24.6 CH_3	24.5 CH_3
13′	24.7 CH_3	24.9 CH_3	24.7 CH_3	24.7 CH_3	24.6 CH_3	24.5 CH_3
14′	13.0 CH_3	13.09 CH_3	13.0 CH_3	12.9 CH_3	13.0 CH_3	12.9 CH_3
15′	25.9 CH_3	25.3 CH_3	25.7 CH_3	25.7 CH_3	26.0 CH_3	25.5 CH_3
1″	124.97 qC	126.0 qC	126.0 qC	144.2 qC	126.1 qC	126.1 qC
2″	139.6 CH	139.7 CH	139.5 CH	128.0 CH	137.6 CH	137.9 CH
3″	125.02 qC	124.qC	124.7 qC	148.4 qC	124.8 qC	124.7 qC
4″	134.0 CH	134.3 CH	133.9 CH	114.4 CH	133.5 CH	133.4 CH
5″	144.84 qC	140.3 qC	140.3 qC	151.2 qC	139.7 qC	139.5 qC
6″	135.20 CH	135.7 CH	134.9 CH	132.0 CH	134.7 CH	134.6 CH
7″	127.01 CH	127.2 CH	126.8 CH	195.1 CH	127.3 CH	127.2 CH
8″	145.42 qC	145.5 qC	145.5 qC	134.4 qC	144.3 qC	144.2 qC
9″	132.93 qC	132.7 qC	132.7 qC	131.8 qC	132.5 qC	132.7 qC
10″	138.85 qC	137.8 qC	137.8 qC	141.4 qC	137.9 qC	137.7 qC
11″	37.96 CH	37.5 CH	37.5 CH	28.8 CH	37.6 CH	37.6 CH
12″	24.7 CH_3	24.9 CH_3	24.7 CH_3	24.2 CH_3	24.6 CH_3	24.6 CH_3
13″	24.7 CH_3	24.9 CH_3	24.7 CH_3	24.3 CH_3	24.6 CH_3	24.6 CH_3
14″	12.9 CH_3	13.1 CH_3	12.9 CH_3	12.9 CH_3	13.2 CH_3	13.4 CH_3
15″	26.8 CH_3	26.4 CH_3	26.7 CH_3	17.3 CH_3	27.4 CH_3	27.3 CH_3
OCH3		52.8 CH_3				
		53.3 CH_3				

[a]Measured in $CDCl_3$. [b]Measured in DMSO-d_6.

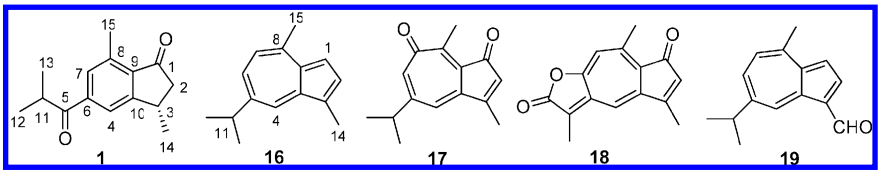

Figure 1. Structures of anthogorgiene A (**1**) and the known monomers.

Anthogorgiene C (**3**) has a molecular formula of $C_{30}H_{32}O_2$ as determined by a quasimolecular ion peak at m/z 425.2462 $[M + H]^+$ in its HRESIMS spectrum. Its NMR spectroscopic data closely resembled those of **2**, except for the substituent at C-4. The presence of an isobutanoyl unit was evident from the protons of two methyl group (δ_H 1.28, J = 6.8 Hz, 6H)

dx.doi.org/10.1021/jf2040862 | J. Agric.Food Chem. 2012, 60, 112−123

Scheme 1. Biogenetic Relationship of the Isolated Compounds

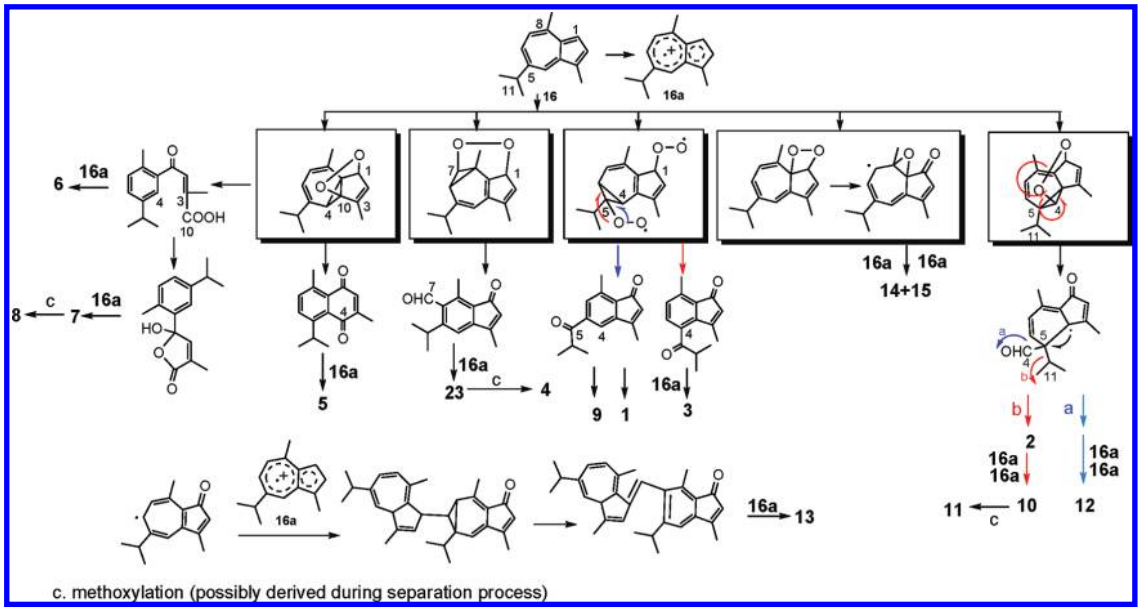

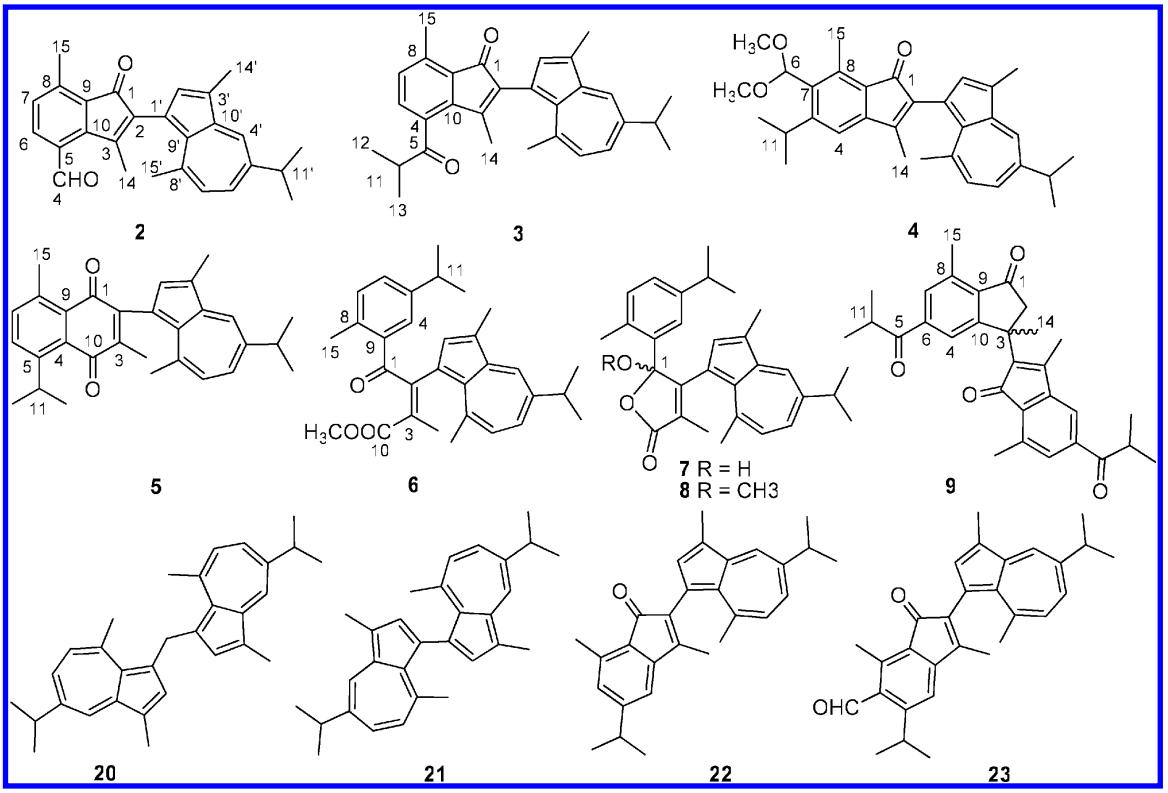

Figure 2. Structures of anthogorgienes B–I (**2**–**9**) and known dimers.

correlated to an aliphatic methine (δ_H 3.32, dq, J = 6.8 Hz) in ^{1}H–^{1}H COSY and interacted with a ketone (δ_C 209.0, C-5) in HMBC. This group was deduced to be positioned at C-4 on the basis of the HMBC relationship between H-6 (δ_H 7.26) and C-5. The indenone unit of **3** was suggested to be derived from the same intermediate of **1**, but bond cleavage occurred at C-5/C-6 instead of C-4/C-5.

A comparison of NMR data revealed anthogorgiene D (**4**) to be an analogue of **23**. The difference was due to the presence of a dimethoxymethane, which was evident from the signals of overlapped methoxy protons at δ_H 3.38 (6H, s) and an acetal proton at δ_H 5.58 (1H, s, H-7) in association with their HMBC interactions. This unit was deduced to be located at C-6 on the basis of the HMBC interactions from H-7 to C-5 (δ_C 154.4), C-6 (δ_C 135.1), and C-8 (δ_C 136.5). Conversion of **4** to **23** under 100 °C in DMSO (Figure 3) further confirmed the structural assignment.

The NMR (Tables 1 and 2) and HRESIMS data (m/z 425.2462 [M + H]$^+$) indicated that anthogorgiene E (**5**) was a guaiazulene-containing dimer. Analysis of 2D NMR (^{1}H–^{1}H COSY, HMQC, and HMBC) data revealed **5** to possess the same substituted guaiazulenyl unit as **2**–**4**. The rest was in

dx.doi.org/10.1021/jf2040862 | J. Agric.Food Chem. 2012, 60, 112–123

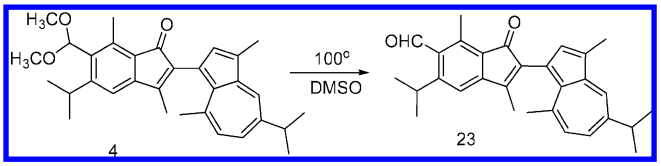

Figure 3. Conversion of **4** to **23**.

accordance with a naphthoquinone nucleus, which was recognized from the resonances for two unsaturated ketones (δ_C 187.9 and 189.3) in addition to eight sp^2 carbons. Except for the substituents located at the guaiazulenyl unit, NMR spectra presented an additional two methyl groups and an isopropyl group. The NOE interactions between H-7 (δ_H 7.47, d, J = 7.5 Hz) and H_3-15 (δ_H 2.67, s) and between H-6 (δ_H 7.65, d, J = 7.5 Hz) and isopropyl methine (δ_H 4.21), in combination with HMBC correlations from H_3-14 (δ_H 2.00) and H-6 to a ketone (δ_C 189.3) confirmed C-5 to be linked by isopropyl group, whereas C-3 and C-8 were thus substituted by methyl groups. The connection of naphthoquinone to the guaiazulenyl unit via a C-2 and C-1′ bond was deduced by the HMBC correlations of H-2′ and H_3-14 to C-2 (δ_C 144.0).

The naphthoquinone nucleus of **5** was speculated to be derived from guaiazulene followed by a C-1 and C-10 peroxidated intermediate and then cleavage of the C-9/C-10 bond in a 4,9,10-cyclopropane to form a C-9/C-4 bond (Scheme 1).

Anthogorgiene F (**6**) was obtained as a green amorphous powder. Its HRESIMS data gave a pseudomolecular ion peak at m/z 457.2722 $[M + H]^+$ (calcd 457.2743) in positive-ion mode, corresponding to the molecular formula of $C_{31}H_{36}O_3$ and indicating 14° unsaturation. The ^1H NMR and APT spectroscopic data indicated **6** also contained a guaiazulenyl unit. Moreover, the ^1H NMR spectrum exhibited a phenyl ABX spin system at δ_H 7.76 (1H, d, J = 1.5 Hz, H-4), 7.13 (1H, d, J = 8.0 Hz, H-7), and 7.22 (1H, dd, J = 1.5, 8.0 Hz, H-6) for a trisubstituted phenyl ring, along with a methyl and an isopropyl group, whereas the HMBC correlations of H_3-12 and H_3-13 (δ_H 1.27) to C-5 (δ_C 145.6) and of H_3-15 (δ_H 2.47) to C-7 (δ_C 131.8), C-8 (δ_C 137.3), and C-9 (δ_C 135.8) clarified the substitution of a methyl group at C-8 and an isopropyl group at C-5. The remaining resonances consisted of a ketone (δ_C 198.3, C-1), two olefinic carbons, C-2 and C-3 (δ_C 131.4, 149.6), a carboxylic carbon (δ_C 168.6, C-10), a methoxy group (δ_C 51.8, δ_H 3.56), and a methyl group, H_3-14 (δ_C 17.0, δ_H 1.85). The HMBC relationships from H_3-14 to C-10, C-3, and C-2 and a weak correlation to C-1, together with the relationship between methoxy protons and C-10, led to the assignment of a 2-methyl-4-oxobut-2-enoic methylate. Additional HMBC correlations from H-4 to C-1 and from H-2′ to C-2 confirmed the linkage of this unit to the phenyl ring and guaiazulenyl unit via C-1/C-9 and C-2/C-1′ bonds. In a NOE difference experiment, the NOE interaction between H_3-14 and H_3-15′ led to the assignment of 2Z geometry.

Comparison of NMR spectroscopic data (Tables 1 and 2) disclosed anthogorgiene G (**7**) sharing the same partial structure as **6** with respect to guaiazulenyl and phenyl units. Further analysis of NMR data revealed **7** to contain the third subunit closely related to **6**, with the exception of an acetal carbon (δ_C 107.1, C-1) to replace a ketone of **6**. In the HMBC spectrum, H_3-14 (δ_H 1.73) correlated to C-10 (δ_C 172.9, C-10), C-2 (δ_C 159.4), and C-3 (δ_C 127.7) and weakly correlated to C-1, in association with the molecular unsaturation, establishing an α,β-unsaturated γ-lactone. The unit connectivity was determined to be the same at that of **6**, on the basis of the HMBC relationships and NMR data similar to those of **6**. The measured optical rotation value (zero) and the absence of Cotton effects suggested **7** to be a racemic mixture. Thus, **7** is designated (±)-anthogorgiene G.

Anthogorgiene H (**8**) was determined as a C-1 methoxylated analogue of **7**, on the basis of the close similarity of their NMR data and the presence of a methoxy group and its protons showing HMBC correlation to C-1 (δ_C 110.8) in association with its molecular weight being 14 amu more than that of **7**. Like the case of **7**, compound **8** also showed zero value of rotation and no Cotton effect, suggesting **8** to be a racemic mixture and, thus, its designation of (±) anthogorgiene H.

Anthogorgiene I (**9**) had a molecular formula of $C_{30}H_{32}O_4$ as determined by a quasimolecular ion peak at m/z 479.2192 $[M + Na]^+$ in HRESIMS. Analysis of 2D NMR data and comparison of its NMR data with these of **1** revealed **9** to consist of two subunits, which were identified as a 3,8-dimethyl-6-isobutanoylindanone and a 3′,8′-dimethyl-6′-isobutanoyindenone. The indanone unit was determined on the basis of the presence of methylene H_2-2 (δ_H 2.78, 3.14, d, J = 19.0 Hz) in addition to the HMBC interactions from H_3-14 (δ_H 1.87) to C-10 (δ_C 162.7), C-2 (δ_C 58.3), and a quaternary carbon C-3 (δ_C 42.4, qC), indicating C-3 to be bonded by the second subunit. The NMR data of the indenone unit were mostly identical to those of **1**, except for C-2′, which presented a quaternary carbon (δ_C 136.5) instead of an olefinic methine. The linkage of two subunits via a C-3/C-2′ bond was confirmed by the HMBC interactions from H_3-14 to C-2′. The lack of rotation and CD effect suggested **9** also presented as a racemic mixture, thus designated (±)-anthogorgiene I.

Anthogorgienes J–O (**10**–**15**) were classified into trimeric patterns. These compounds featured the substitution of two guaiazulenyl units to an oxidated guaiazulene with the exception of **13**n which contained two oxidated subunits.

Anthogorgiene J (**10**) was obtained as a purple amorphous powder. Its molecular formula was determined as $C_{42}H_{42}O_2$ on the basis of HRESIMS (m/z 625.3668 $[M + H]^+$) data, requiring 22° unsaturation. The IR absorptions at 1706 and 1682 cm^{-1} in association with ^{13}C NMR data indicated the presence of two carbonyl groups. Its ^{13}C NMR and APT spectra exhibited 28 sp^2 carbons in addition to 10 methyl groups, an aldehydic carbon (δ_C 190, CH), and a ketone (δ_C 197.9, qC). Thus, the structure of **10** was assumed to be a highly conjugated polyene. Comparison of NMR data (Tables 3 and 4) revealed that **10** contained two guaiazulenyl units. Analysis of ^1H–^1H COSY and HMBC data (Figure 4) revealed the remaining eight sp^2 carbons together with

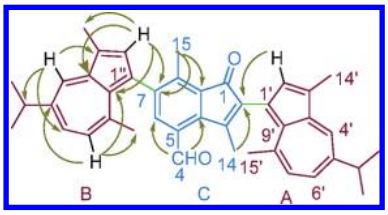

Figure 4. Key HMBC correlations of **10**.

an conjugated ketone (δ_C 197.9, C-1) belonging to an indenone nucleus. The substitution of methyl groups at C-3 and C-8 like that of **2** was evident from the HMBC correlations from H_3-14 (δ_H 2.46, s) to C-10, C-3 (δ_C 151.4), and C-2 (δ_C 140.3), and a weak correlation to C-1, and from H_3-15 to C-7, C-8, and C-9.

dx.doi.org/10.1021/jf2040862 | J. Agric.Food Chem. 2012, 60, 112–123

The HMBC relationship between H-6 (δ_H 7.84, s) and aldehydic carbon (δ_C 190.0, C-4) along with the NOE relationship between the aldehydic proton H-4 (δ_H 10.70, s) and H_3-14 (δ_H 2.46, s) ascertained the aldehydic group linked to C-5. The proton singlet H-6 and the absence of H-2 suggested C-7 and C-2 to be substituted. Their assignments were confirmed by the HMBC correlations from H-6 to C-1″ and from H-2′ to C-2 to establish C-1′/C-2 and C-1″/C-7 connectivities.

The NMR spectroscopic data of anthogorgiene K (**11**) closely resembled those of **10**. The distinction was due to the substitution at C-5, where two MeO signals (δ_H 3.31 and 3.29) and an acetal methine CH-5 (δ_H 5.87, δ_C 99.8) were observed to replace an aldehydic group of **10**. On the basis of the HMBC interactions from acetal proton H-4 to C-10 (δ_C 143.5), C-6 (δ_C 133.6), C-5 (δ_C 142.0), and methoxy carbons, a dimethoxymethyl group was deduced to be substituted at C-4. Thus, **11** was determined as a C-4 dimethoxylated product of **10** (Figure 5).

For anthogorgiene L (**12**), the close similarity of NMR data indicated that it is an analogue of **10**, except for the presence of a singlet for two methyl group (δ_H 1.74, s, 6H) and a hydroxylated quaternary carbon (δ_C 72.7, C-11), which were assigned to a 2-hydroxyisopropyl group on the basis of their HMBC relationships. Further HMBC correlations from the methyl protons (δ_H 1.74, s) to C-11 and C-5 (δ_C 142.0) confirmed C-5 to be substituted by a 2-hydroxyisopropyl group.

Analysis of the oxidative mechanism (Scheme 1) suggested that **12** and **10** share the same intermediate, but **10** maintained C-4 to form an aldehydic group in contrast to **12**, which lost C-4 to keep an isopropyl group. The hydroxylation at C-11 of **12** was speculated to undergo at last step of oxidation. This assumption was partly supported by the isolation of 11-hydroxyguaiazulene-3-carbaldehyde from a mushroom, *Lactarius hatsudake*.[23]

Anthogorgiene M (**13**) gave a molecular formula of $C_{45}H_{48}O_2$ as established by HRESIMS data, indicating 22° unsaturation. Its ^{1}H and ^{13}C NMR features were closely related to those of **10**, containing 28 sp^2 carbons in addition to 12 methyl groups and an aldehydic group. The ^{1}H−^{1}H COSY correlations indicated the presence of three isopropyl groups. Analysis of 1D and 2D NMR spectroscopic data and comparison of NMR data with those of **10**−**12** resulted in a trimeric backbone, containing a monosubstituted guaiazulene, and two indenone units (units B and C). HMBC data connected units A and B to form a guaiaiazulenylindenone, the NMR data of which were almost identical to those of **23** with the exception of the substitution at C-6. For unit C, its NMR data were closely related to those of unit B. An aldehydic group to be positioned at C-6″ was deduced on the basis of HMBC relationship of the aldehydic proton (δ_H 10.80, H-7″). However, C-1″ of unit C was assigned to a quaternary olefinic carbon (δ_C 144.2) rather than a ketone. The fact that a methine proton (δ_H 7.48, s, H-7) correlated to C-2″ (δ_C 128.0), C-1″, and C-9″ (δ_C 131.8), in addition to the HMBC relationship between H-2″ (δ_H 6.19, s) and C-7 (δ_C 129.2) (Figure 6), clarified the

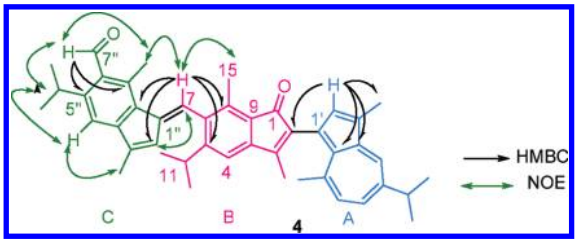

Figure 6. Key HMBC and NOE correlations of **13**.

connection of units B and C via a C-7 bridge. In the NOE experiment, irradiation of H-7 induced the enhancement of H_3-15″, indicating $\Delta^{1'',7}$ to be in *E* geometry.

Anthogorgienes N (**14**) and O (**15**) were separated by a chiral HPLC chromatography using an OD-RH column.

The molecular formula of anthogorgiene N (**14**) was determined as $C_{45}H_{50}O_2$ on the basis of HRESIMS (*m*/*z* 623.3869 $[M + H]^+$) and NMR data, indicating 21° unsaturation. Its ^{1}H and ^{13}C NMR spectroscopic data (Tables 3 and 4) in association with MS data featured a guaiazulene-based trimer. The presence of two monosubstituted guaiazulenyl units (A and C) was recognized by the close similarity of NMR data in comparison with those of guaiazulene. The NMR data of unit B also presented guaiazulenyl features, whereas the distinction was due to the presence of a ketone (δ_C 199.0, C-1) and two oxygenated carbons at δ_C 65.8 (C-9) and 80.3 (C-8), in addition to an aliphatic methine CH-7 (δ_H 5.09. δ_C 45.6). In the ^{1}H−^{1}H COSY spectrum, the relationships between H-7 (δ_H 5.09, *J* = 11.2 Hz) and an olefinic proton H-6 (δ_H 5.96, *J* = 11.2 Hz) and the HMBC correlations from H-7 to C-5, C-8, C-9, and also C-15, together with a weak HMBC correlation between H_3-14 and a ketone carbon C-1, led to the assignment of a ketone at C-1, whereas an 8,9-epoxide was assigned on the basis of the molecular unsaturation. The connectivity from unit B to units A and C was determined by further HMBC

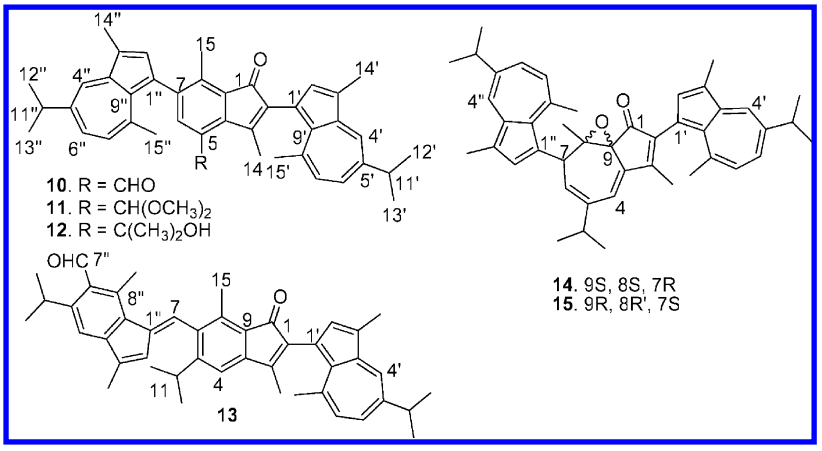

Figure 5. Structures of anthogorgienes J−O (**10**−**15**).

dx.doi.org/10.1021/jf2040862 | *J. Agric.Food Chem.* 2012, 60, 112−123

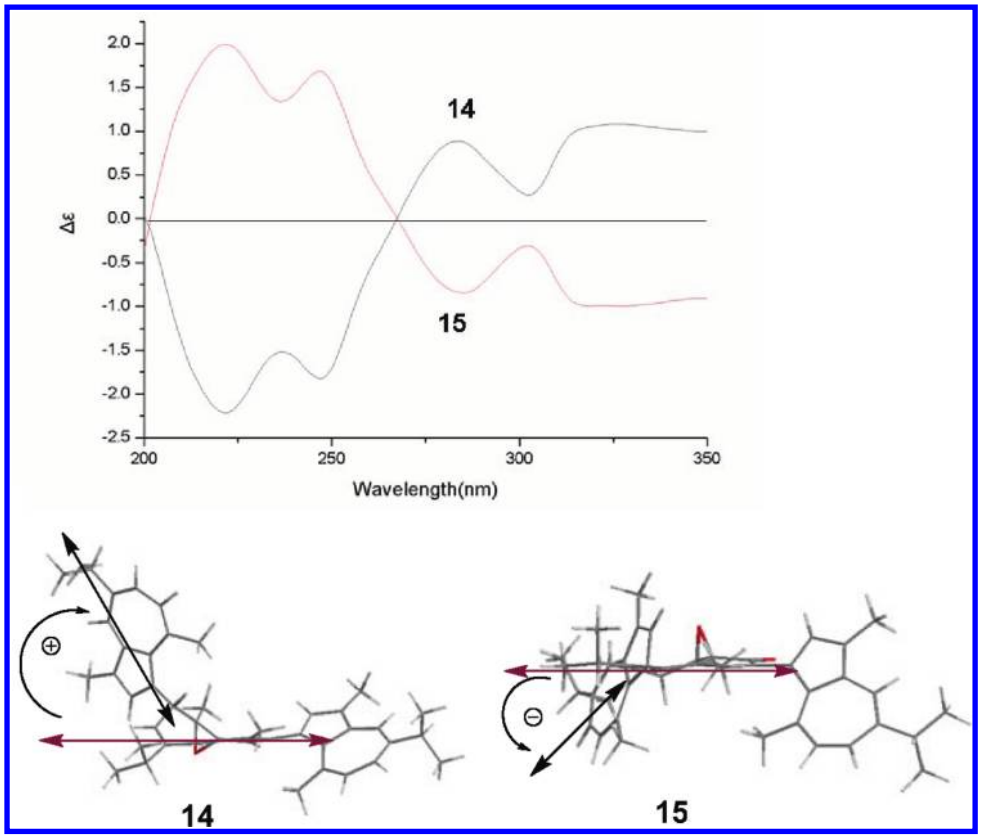

Figure 7. CD spectra of **14** (blue line) and **15** (red line).

correlations from H-2′ and H_3-14 to C-2 and from H-7 to C-1″, C-2″, and C-9″, indicating the formation of C-1′/C-2 and C-7/C-1″ bonds. The NOE relationship between H-7 and H_3-15 suggested them to be oriented in the same face.

The absolute configuration of **14** was elucidated by the exciton chirality method.[26] Because the dimers such as **3** and **5** with two chromophores showed weak Cotton effect (Supporting Information) due to the free axial rotation, the Cotton effects centered at UV peaks 280 and 250 nm of **14** were regarded as arising from the interaction of the chromophores of units C and B. The positive sign of the first Cotton effect at λ_{max} 280 nm and the negative sign of the second one at λ_{max} 250 nm indicated the chirality centered at C-7 to adopt a right-handed screw (Figure 7). Therefore, the configuration of C-7 was assumed to be *R*. Accordingly, the remaining chiral centers were assigned to 9*S* and 8*S*.

The duplicated NMR data of anthogorgiene O (**15**) in comparison with those of **14**, assisted by the rotation sign of **15** ($[\alpha]_D^{20}$ −950.3, MeOH) being in contrast to the value of **14** ($[\alpha]_D^{20}$ +842.8, MeOH), indicated **15** to be an enantiomer of **14**. The opposite Cotton effects of **15** and **14** (Figure 7) further supported this assignment.

Oxidation of guaiazulene to generate various oxidated and ring-rearranged derivatives and the reaction mechanism were intensively studied. For example, the monomers 1,7-guaiazulenequinone (**17**) and the aldehydic analogue (**19**), together with dimers (**20**−**23**), were reported to be derived from guaiazulene in DMF at 100 °C. However, ketolactone (**18**) as formerly isolated from a deep sea gorgonian was regarded to be a genuine natural product. To determine whether our isolated compounds were a group of artifacts derived by oxidation of guaiazulene, the frozen sample was dried under vacuum and then extracted by MeOH. The MeOH extract was subsequently detected by HPLC (ODS) and ^{1}H NMR spectrum. Fortunately, the spectroscopic features covered most isolated compounds with the exception of some overlapped signals remaining uncertain. Thus, we assumed that the most analogues were derived from guaiazulene by ecological conditions rather than by separation process. However, **4** and **11** are suspected to be artifacts derived during the separation process. The conversion relationships of the compounds were postulated as shown in Scheme 1. Co-occurrence of monomers to trimers in the specimen represented the stages of condensation when guaiazulene was oxidated to radical cation (**16a**) as induced by molecular oxygen.[18] It is noteworthy that the oxidation and condensation are mostly

Table 5. Effects of Compounds against Larval Settlement of *Balanus amphitrite*

	B. amphitrite	
compd	EC_{50} (μg/mL)	LC_{50} (μg/mL)
16	16.98	>50
19	2.13	>50
18	6.69	>50
17	2.67	>50
7	5.92	>50
2	>25	UD[a]
20	>25	UD
21	>25	UD
22	>25	UD
23	>25	UD
14	>25	UD
15	>25	UD

[a]Undetectable.

dx.doi.org/10.1021/jf2040862 | *J. Agric.Food Chem.* 2012, 60, 112−123

Table 6. Antimicrobial Activities of Guaiazulene Derivatives

	IC_{50} (μg/mL)				
compd	*A. fumigatus*	*A. flavus*	*F. oxysporum*	*S. aureus*	*S. pneumoniae*
7	>50	>50	>50	18.03 ± 0.80	12.67 ± 0.32
17	13.34 ± 2.52	18.68 ± 0.76	15.04 ± 0.38	12.30 ± 1.36	15.66 ± 0.40
19	19.50 ± 0.12	37.90 ± 0.85	35.50 ± 1.01	>50	>50
amphotericin B				0.021 ± 0.003	1.58 ± 0.06
ampicillin	4.15 ± 0.80	0.40 ± 0.01	0.99 ± 0.05		

susceptible to position C-1. Most dimers and trimers are likely formed by the radical reaction of radical cation (**16a**) with the oxidated product such as indenone except for **13**, in which the radical position C-7 of the 1-oxidated intermediate reacted with the second guaiazulene instead of the oxygen atom.

Some of the compounds were selected for antifouling tests. The oxidated monomers **17**−**19** and dimer **7** showed significant inhibition against the larval settlement of barnacle *B. amphitrite* with EC_{50} < 7.0 μg/mL, whereas guaiazulene and others were weak against the larval settlement (EC_{50} > 25 μg/mL) (Table 5). These findings implied guaiazulene-derived products partly play the role of ecological functions.

In addition, nine compounds representing monomers (**16**, **17**, **19**), dimers (**7**, **21**−**23**), and trimers (**14**, **15**) were selected for antibiotic tests. The bioassay results revealed the moderate inhibition of **17** against *Aspergillus fumigatus*, *Aspergillus flavus*, *Fusarium oxysporum*, *Staphylococcus aureus*, and *Staphylococcus pneumoniae*, whereas **19** showed moderate inhibition toward *A. fumigatus*, *A. flavus*, and *F. oxysporum*, and **7** showed selective inhibition against *S. aureus* and *S. pneumoniae* (Table 6).

This is a first report of naturally occurring guaiazulenyl trimers from marine organisms, and this work also provides a new gorgonian genus to derive a rich guaiazulene-based analogues. The diverse polyazulenes are currently drawing increasing interest because of the potential utility of their physicochemical properties as well as biological activity.

■ ASSOCIATED CONTENT

Supporting Information

1D and 2D NMR, IR, and MS spectra for anthogorgienes A−O (**1**−**15**). This material is available free of charge via the Internet at http://pubs.acs.org.

■ AUTHOR INFORMATION

Corresponding Author

*Phone: (86)10-82806188. Fax: (86)10-82802724. E-mail: whlin@bjmu.edu.cn.

Funding

This work was supported by grants from the NSFC (No. 30930109), the National Key Innovation Project (2009ZX09501-014, 2009ZX09103-140, 201005022-4), and the International Cooperation Projects (2010DFA31610).

■ REFERENCES

(1) Chambers, L. D.; Stokes, K. R.; Walsh, F. C.; Wood, R. J. K. Modern approaches to marine antifouling coatings. *Surf. Coat. Technol.* **2006**, *201*, 3642−3652.

(2) Omae, I. General aspects of tin-free antifouling paints. *Chem. Rev.* **2003**, *103*, 3431−3448.

(3) Fusetani, N. Antifouling marine natural products. *Nat. Prod. Rep.* **2011**, *28*, 400−410.

(4) Limma Mol, V. P.; Raveendran, T. V.; Parameswaran, P. S.; Kunnath, R. J.; Sathyan, N. Antifouling sesquiterpene from the Indian soft coral, Simularia kavarattiensis Alderslade and Prita. *Indian J. Mar. Sci.* **2010**, *39*, 270−273.

(5) Davis, A. R. Alkaloids and ascidian chemical defense: evidence for the ecological role of natural products from *Eudistoma olivaceum*. *Mar. Biol.* **1991**, *111*, 375−379.

(6) Clavico, E. E. G.; Muricy, G.; da Gama, B. A. P.; Batista, D.; Ventura, C. R. R.; Pereira, R. C. Ecological roles of natural products from the marine sponge *Geodia corticostylifera*. *Mar. Biol.* **2006**, *148*, 479−488.

(7) Qian, P.; Xu, Y.; Fusetani, N. Natural products as antifouling compounds: recent progress and future perspectives. *Biofouling* **2010**, *26*, 223−234.

(8) Imre, S.; Thomson, R. H.; Yalhi, B. Linderazulene, a new naturally occurring pigment from the gorgonian *Paramuricea chamaeleon*. *Experientia* **1981**, *37*, 442−443.

(9) Fusetani, N.; Matsunaga, S.; Konosu, S. Bioactive marine metabolites I. isolation of guaiazulene from the gorgonian *Euplexaura erecta*. *Experientia* **1981**, *37*, 680−681.

(10) Okuda, R. K.; Klein, D.; Kinnel, R. B.; Li, M.; Scheuer, P. J. Marine natural products: the past twenty years and beyond. *Pure Appl. Chem.* **1982**, *54*, 1907−1914.

(11) Li, M. K. W.; Scheuer, P. J. Halogenated blue pigments of a deep sea gorgonian. *Tetrahedron Lett.* **1984**, *25*, 587−590.

(12) Li, M. K. W.; Scheuer, P. J. A. Guaianolide pigment from a deep sea gorgonian. *Tetrahedron Lett.* **1984**, *25*, 2109−2110.

(13) Sakemi, S.; Higa, T. 2,3-Dihydrolinderazulene, a new bioactive azulene pigment from the gorgonian *Acalycigorgia* sp. *Experientia* **1987**, *43*, 624−625.

(14) Tanaka, J. I.; Miki, H.; Higa, T. Echinofuran, a new furanosesquiterpene from the gorgonian *Echinogorgza praelonga*. *J. Nat. Prod.* **1992**, *55*, 1522−1524.

(15) Ochi, M.; Kataoka, K.; Tatsukawa, A.; Kotsuhi, H.; Shibata, K. Gorgiabisazulene and gorgiagallylazulene, two new guaiazulenoid pigments from a gorgonian *Acalycigorgia* sp. *Chem. Lett.* **1993**, 2003−2006.

(16) Seo, Y.; Rho, J. R.; Geum, N.; Yoon, J. B.; Shin, J. Isolation of guaianoid pigments from the gorgonian *Calicogorgia granulosa*. *J. Nat. Prod.* **1996**, *59*, 985−986.

(17) Aknin, M.; Rudi, A.; Kashman, Y.; Gaydou, E. M. Bebryazulene, a new guaiane metabolite from the Indian ocean gorgonian coral. *Bebryce grandicalyx*. *J. Nat. Prod.* **1998**, *61*, 1286−1287.

(18) Reddy, N. S.; Reed, J. K.; Longley, R. E.; Wright, A. E. Two new cytotoxic linderazulenes from a deep-sea gorgonian of the genus *Paramuricea*. *J. Nat. Prod.* **2005**, *68*, 248−250.

(19) Manzo, E.; Ciavatta, M. L.; Gresa, M. P. L.; Gavagnin, M.; Villani, G.; Naik, C. G.; Cimino, G. New bioactive hydrogenated linderazulene-derivatives from the gorgonian *Echinogorgia complexa*. *Tetrahedron Lett.* **2007**, *48*, 2569−2571.

(20) Kapustina, I. I.; Kalinovskii, A. I.; Grebnev, B. B.; Savina, A. S.; Stonik, V. A. Sesquiterpenoids from the far-eastern gorgonaria *Stenogorgia* sp. *Chem. Nat. Compd.* **2009**, *45*, 916−917.

(21) Matsubara, Y.; Takekuma, S.; Yokoi, K.; Yamamoto, H.; Nozoe, T. Autoxidation of guaiazulene and 4,6,8-trimethylazulene in polar aprotic solvent: structural proof for products. *Bull. Chem. Soc.* **1987**, *60*, 1415−1428.

(22) Takekuma, S.; Matsubara, Y.; Yamamoto, H.; Nozoe, T. Autoxidation of solid guaiazulene and of the solution in DMF in the presence of base or acid: a comparative study of the product distribution. *Bull. Chem. Soc.* **1988**, *61*, 475−481.

(23) Thiyagarajan, V.; Harder, T.; Qian, P. Y. Combined effects of temperature and salinity on larval development and attachment of the subtidal barnacle *Balanus trigonus* Darwin. *J. Exp. Mar. Biol. Ecol.* **2003**, *287*, 223−236.
(24) Dobretsov, S.; Xiong, H. R.; Xu, Y.; Levin, L. A.; Qian, P. Y. Novel antifoulants: inhibition of larval attachment by proteases. *Mar. Biotechnol.* **2007**, *9*, 388−397.
(25) Li, E.; Jiang, L.; Guo, L.; Zhang, H.; Che, Y. Pestalachlorides A−C, antifungal metabolites from the plant endophytic fungus *Pestalotiopsis adusta*. *Bioorg. Med. Chem.* **2008**, *16*, 7894−7899.
(26) Hansen, H. J.; Sliwka, H. R.; Hug, W. The absolute configuration of 1-methylindane. *Helv. Chim. Acta* **1979**, *62*, 1120−1128.
(27) Tada, M.; Moriyama, Y.; Tanahashi, Y.; Takahashi, T. Absolute stereochemistry of farfugin A. *Bull. Chem. Soc.* **1975**, *48*, 549−552.